ChemComm

COMMUNICATION

View Article Online
View Journal | View Issue

Cite this: *Chem. Commun.*, 2023, 59, 466

Received 28th November 2022,
Accepted 5th December 2022

DOI: 10.1039/d2cc06285b

rsc.li/chemcomm

Dual and sequential locked/unlocked photo-switching effects on FRET processes by tightened/loosened nano-loops of diarylethene-based [1]rotaxanes†

Trang Manh Khang,[a] Pham Quoc Nhien,[ab] Tu Thi Kim Cuc,[a] Chia-Hua Wu,[a] Bui Thi Buu Hue,[b] Judy I. Wu,[c] Yaw-Kuen Li[de] and Hong-Cheu Lin*[ae]

The self-trapping nano-loop structures of [1]rotaxanes exhibited multiple Förster resonance energy transfer (FRET) patterns *via* dual and sequential locking/unlocking of pH-gated and UV exposure processes. As a tightened and constrained nano-loop in the acidic condition, dithienylethene (DTE) unit was locked in the highly bending open form to forbid ring closure upon UV irradiation.

Recently, mechanically interlocked molecules (MIMs) with 3-dimensional architectures have attracted considerable interest in the development of molecular switches and machines.[1–3] Several studies have investigated the controlling and switching quasi-mechanical motion of MIMs with certain external stimuli, including redox, pH, light and temperature, providing nanoscale devices for the fabrication of actuators, switches, motors and nanites.[4–8] Among them, the bistable [2]rotaxane as a representative example of MIMs contains a host macrocycle interlocked onto another linear guest dumbbell by supramolecular interactions,[9,10] while the [1]rotaxane molecular structure is a single molecular system with the combination of host and guest moieties together to self-trap the axle tail inside its own macrocycle head.[11–13] Interestingly, the reciprocating shuttling motion of the macrocycle causes rigorous changes between contraction and extension configurations of [1]rotaxane isomers, leading to the obvious reduction in the rotation of rotors due to the bulky steric hindrance of the self-tightened structure.[14–16] Along with potential applications of rotaxanes based on molecular shuttling and introducing various specific functionalities with delicate designs into rotaxane structures, the corresponding reversible properties can be tuned easily.[17–19] The development of sophisticated and functional molecules that concede a variety of interactions among their components is desirable, such as energy-, electron- and charge-transfer, *etc.*[19] resulting in controllable molecular devices and machines, which have significant impacts on the improvement of sensing, electronic, nanotechnological and biological applications.[20–24]

Photons are utilized as efficient external triggers for energizing photochromic and photo-switchable molecules.[25,26] Dithienylethene (DTE) and its derivatives are one of the most distinguished optical switching agents since they have optimal effectiveness on customizable functions and exhibit excellent thermal stabilities, fatigue resistances and photo-conversion efficiencies.[27] In addition, Förster resonance energy transfer (FRET) phenomena, as a non-radiative energy transfer process from an excited-state donor to an acceptor in the ground state through dipole–dipole coupling, rely on an appreciable overlap of the donor emission with acceptor absorption spectra and a suitable donor–acceptor distance.[28] Thus, a considerable number of FRET-based materials have been prepared by the combination of various photochromic and fluorophoric donors–acceptors in covalent and supramolecular systems.[29,30] A notable example of this strategy is tetraphenylethane (TPE) as an aggregation-induced emission (AIE) donor and DTE as a photochromic acceptor to control *in vivo* imaging and cancer surgery to display many unique characteristics as smart systems with benefits at higher levels of molecular design.[31]

Numerous concepts of gated photochromism of DTE derivatives have successfully proceeded through non-covalent interactions including host–guest supramolecules, multiple hydrogen bonds, π–π stacking and so forth.[32,33] However, the naked-eye colour changes in these systems are inferior to the visualization of photo-switchable fluorescence materials. Hence, we designed and investigated novel multi-stimuli

[a] *Department of Materials Science and Engineering, National Yang Ming Chiao Tung University, Hsinchu 300, Taiwan. E-mail: linhc@nycu.edu.tw*
[b] *Department of Chemistry, College of Natural Sciences, Can Tho University, Can Tho City, Vietnam*
[c] *Department of Chemistry, University of Houston, Houston, Texas 77204, USA*
[d] *Department of Applied Chemistry, National Yang Ming Chiao Tung University, Hsinchu 300, Taiwan*
[e] *Center for Emergent Functional Matter Science, National Yang Ming Chiao Tung University, Hsinchu 300, Taiwan*

† Electronic supplementary information (ESI) available. See DOI: https://doi.org/10.1039/d2cc06285b

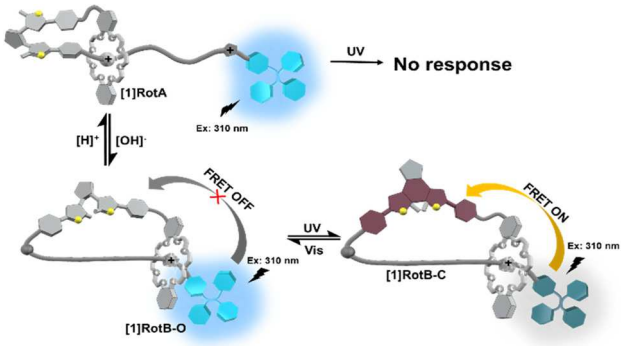

Fig. 1 Schematic representation of controllable FRET behaviors between TPE and DTE units under acid–base reversible processes between **[1]RotA** and **[1]RotB-O** along with reversible photoisomerization processes between **[1]RotB-O** and **[1]RotB-C**.

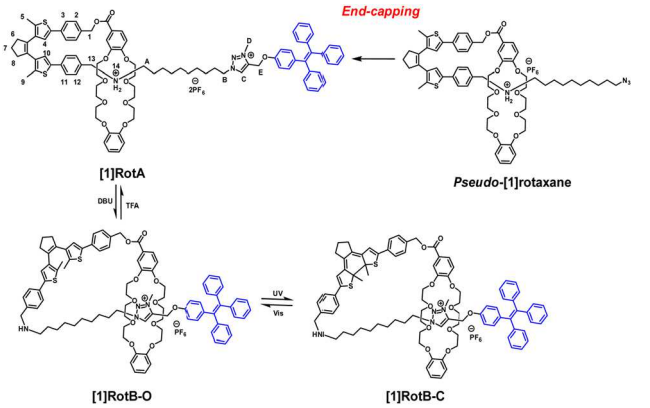

Scheme 1 Synthetic strategies of self-tightened [1]rotaxanes, including **[1]RotA**, **[1]RotB-O** and **[1]RotB-C**.

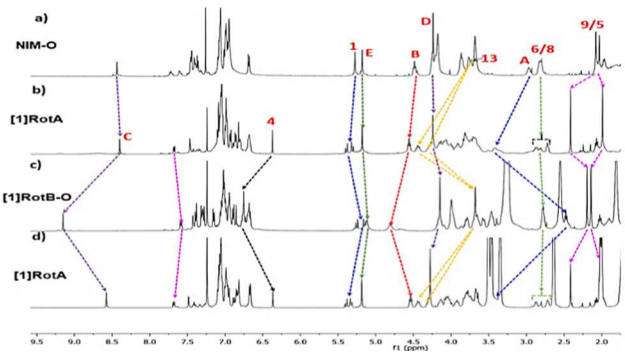

Fig. 2 Partial ^{1}H NMR spectra (500 MHz, $CDCl_3$, 298 K) of (a) **NIM-O**, (b) **[1]RotA**. (c) **[1]RotB-O** (upon the addition of 1.1 equiv. DBU) and (d) **[1]RotA** (upon the further addition of 2.2 equiv. TFA to the solution of (c)).

responsive MIMs incorporating the optical switching DTE unit, as described in Fig. 1, which performed FRET behaviour by integration of the TPE unit as an AIEgen donor and the DTE moiety as a photochromic acceptor in [1]rotaxane. The acid–base controlled shuttling of the macrocycle between distinct stations led to the transformed DTE configurations between parallel (p) and antiparallel (ap) conformers, which demonstrated a gated photochromism due to the locked and non-photoswitchable structure of the p-conformer upon UV irradiation in the acidic condition. Consequently, the pH-gated photochromism behaviour also induced FRET-OFF phenomena, resulting in the photoluminescence (PL) turn-on signals, as illustrated in Fig. 1. Thus, the FRET process can be triggered *via* molecular shuttling by acid/base controls as a programmable molecular machine with multi-stimuli responsiveness.

A photo-switchable interlocked molecule **[1]RotA** was designed and synthesized through the self-tightened molecular strategy using an asymmetrically thread molecule constructed from a dibenzo-24-crown-8 (DB24C8) macrocycle-linked benzylalkylammonium (BAA) station *via* a photochromic DTE bridge and TPE as an AIEgen stopper. Furthermore, compound **[1]RotB-O** with DB24C8 located at the *N*-methyltriazolium (MTA) site was prepared from **[1]RotA** in a base solution of 1,8-diazabicyclo[5.4.0]undec-7-ene (DBU) (see Scheme 1). The synthetic procedures and characterizations of compounds **1–15**, **TPE-propagyl**, [1]rotaxanes and the unthreaded compound (**NIM-O**) are fully described in Fig. S1–S29 and the ESI.† Firstly, the successful synthesis of interlocked **[1]RotA** was proven by the analysis and comparison of the ^{1}H NMR spectra between **[1]RotA** and non-interlocked molecule **NIM** (Fig. 2a and b). Secondly, the reversible motions of **[1]RotA** were examined by ^{1}H NMR spectra under acid and base conditions. As well-known acid–base reagents, trifluoroacetic acid (TFA) and 1,8-diazabicyclo[5.4.0]undec-7-ene (DBU) were used as external stimuli to observe the shuttling of the macrocycle between two distinct binding sites (*i.e.* BAA and MTA stations) of **[1]RotA** and **[1]RotB** (Scheme 1). Besides, the unthreaded behaviour from self-tightened pseudo-[1]rotaxane to linear non-interlocked structures with different synthetic yields of isomeric MIM and NIM structures (45% and 85% for **[1]RotA** and **NIM-C**, respectively) could be controlled by the UV exposure time, as shown in Fig. 3. The details of Scheme 1 and related results of **[1]RotB-O**, **[1]RotB-C**, **[1]RotB-C** + TFA in Fig. S30 are revealed in the ESI.†

In essence, the photochromic DTE unit could undergo reversible photo-isomerization between closed and open forms of DTE-C and DTE-O by UV and Vis light, respectively. Upon different UV irradiation time intervals (at λ_{ex} = 365 nm), the solutions of **[1]RotB-O** and **NIM-O** in DMSO (Fig. S31 and S32b, c, ESI†) produced two new absorption bands at 350–380 (very small absorbance) and 435–680 nm with λ_{max} = 542 nm, so the colour of the solutions was remarkably changed from colourless to purple due to the photochromic behaviour of isomeric DTE structural changes. Nonetheless, **[1]RotA** showed an unexpected UV-inactive behaviour which could be attributed to the *p*-conformer of DTE, resulting in its unaltered optical activity (Fig. S32a, ESI†). As typical AIEgens, [1]rotaxane and related compounds in the DMSO/H_2O system with different water fractions (f_w) were explored in Fig. S33a–f (ESI†), and the solutions of both [1]rotaxanes (**[1]RotA** and **[1]RotB-O**) and the unthreaded compound **NIM-O** in 99% water (DMSO/H_2O = 1/99, v/v) with the strongest AIE behaviours and highest blue PL emission intensities (at 470 nm) were chosen for the other studies.

Interestingly, increasing UV irradiation time, the PL intensities of **[1]RotA** were only decreased slightly, while the original

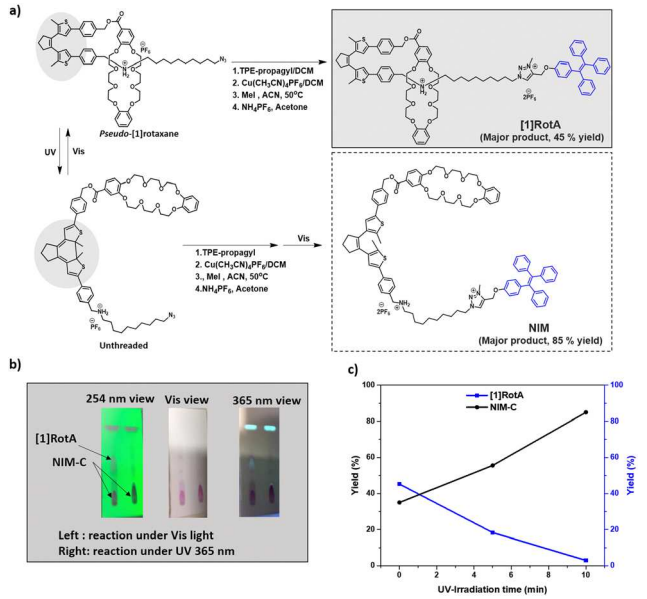

Fig. 3 (a) Synthetic schemes illustrated light-driven processes of pseudo-[1]rotaxane and the unthreaded linear structure controlled by UV/Vis light before the interlocked step. (b) TLC differentiated major productions of isomeric **[1]RotA** and **NIM-C** with DTE-O and DTE-C intermediates under respective Vis and UV exposure conditions. (c) Yields of **[1]RotA** and **NIM-C** controlled by UV irradiation time.

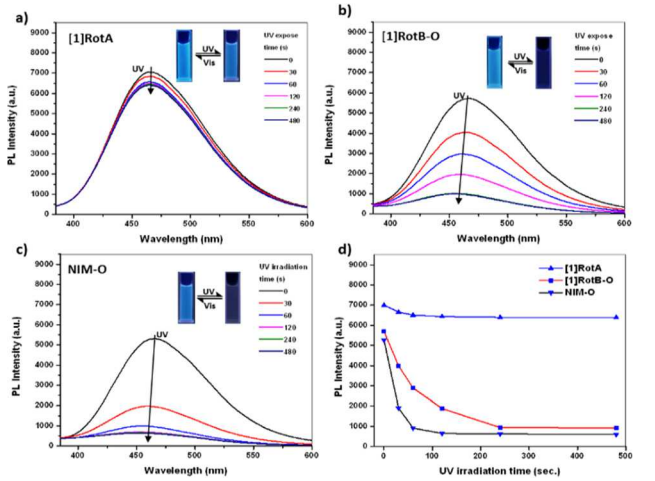

Fig. 4 Time-dependent PL spectra of (a) **[1]RotA**, (b) **[1]RotB-O** and (c) **NIM-O**, and (d) relative emission intensities of **[1]RotA**, **[1]RotB-O** and **NIM-O** at λ_{em} = 470 nm upon UV exposure (0–480 s). Insets: Photographs of fluorescence changes observed in (a) **[1]RotA**, (b) **[1]RotB-O** and (c) **NIM-O** solutions (DMSO/H_2O = 1/99, v/v) before and after UV irradiation. Concentration: 50 μM, λ_{ex}: 310 nm.

blue PL intensities (at 470 nm) of both **[1]RotB-O** and **NIM-O** were remarkably dropped due to converting from the open forms of **[1]RotB-O** and **NIM-O** to the closed forms of **[1]RotB-C** and **NIM-C**, respectively, leading to the activation of the energy transfer through FRET pathways. Thus, the strong blue emissions and open form of DTE were maintained in **[1]RotA** after UV exposure, but the closed form of DTE was obtained and thus the PL emissions in **[1]RotB-C** and **NIM-C** were quenched after UV irradiation (insets of Fig. 4a–c), where **NIM-C** has a more efficient closure time (*ca.* 100 sec.) compared with that (over 200 sec.) of **[1]RotB-C** (loosened loop) after UV exposure (Fig. 4d) due to the higher photo-isomerization rate in **NIM-O** (non-interlocked structure) with the non-constrained open form of DTE. Accordingly, the UV facilitated DTE ring closure reaction speeds and kinetics follow the reversed trend of DTE self-constraint order as: **[1]RotA** (tightened loop) < **[1]RotB-O** (loosened loop) < **NIM-O** (non-interlocked structure). Moreover, their highly reversible photochromic and efficient FRET phenomena along with self-assembly properties in Fig. S34–S37 were verified by SEM, DLS and time-resolved PL (TRPL) measurements (described in the ESI†). To demonstrate the pH-gated FRET phenomena, it is inspired by the pH effects on various photo-switching FRET behaviours (see Fig. S38, ESI†) where bistable [1]rotaxane and related structures (*i.e.*, **[1]RotA**, **[1]RotB** and **NIM-O**) and loosened derivatives were treated by the combinations of base-controlled shuttling (adding DBU) and UV irradiation (365 nm) (described in the ESI†).

To study the rare structural transformations in self-tightened [1]rotaxanes, theoretical calculations were conducted to obtain the optimized structures for different forms of [1]rotaxanes **[1]RotA** (tightened loop) and **[1]RotB** (loosened loop) along with non-interlocked molecule **NIM**. To illustrate their FRET-OFF/ON behaviours, the absorption spectra of isolated closed and open forms of DTE *ap*-conformers were also computed using time-dependent density functional theory (TD-DFT) approaches.[34] The B3LYP/6-31G(d)[35–37] level of theory was employed in this study and all computations were performed using the Gaussian 16 program. The full explications are clearly described in the ESI.† As shown in Fig. 5 and Fig. S39 (ESI†), owing to the largest bending conformation of DTE to induce the larger twisting distance of potentially reactive C1 to C6 for ring closure reaction, the farthest C1 to C6 distance of 5.5 Å in **[1]RotA** was much longer in contrast to those of 3.7 in **[1]RotB-O** and **NIM-O**, and thus the photoisomerization (by UV exposure)

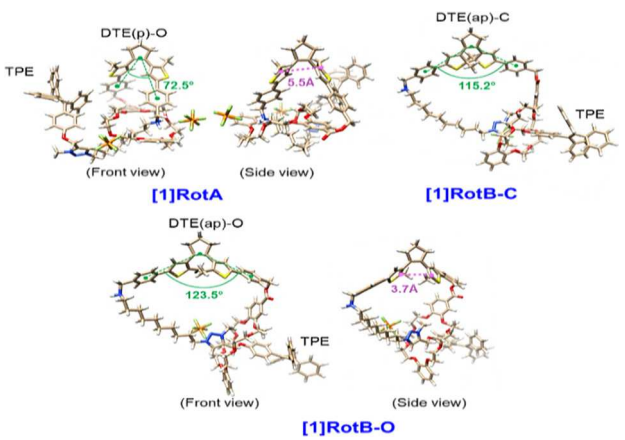

Fig. 5 Optimized structures for **[1]RotA**, **[1]RotB-O** and **[1]RotB-C**; DTE(p) and DTE(ap) refer to parallel- and antiparallel-conformers, while –C and –O indicate the closed and open forms of DTE. The C1 to C6 distances (rC1–C6) for the C1–C6 bond formations in photoisomerization are marked in pink in the side view for open form compounds (**[1]RotA** and **[1]RotB-O**).

was inhibited in this highly bent and constrained structure of **[1]RotA**.

In summary, the dual and sequential locked/unlocked photo-switching effects on reversible FRET processes (under UV/Visible irradiations) were investigated by tightened/loosened nano-loops of diarylethene-based [1]rotaxanes *via* pH-controlled shuttling to the auxiliary methyltriazolium (MTA) binding site. In addition, the unthreaded behaviour from the self-tightened pseudo-[1]rotaxane to linear non-interlocked structures with different synthetic yields of isomeric MIM and NIM structures (45% and 85% for **[1]RotA** and **NIM-C**, respectively) could be controlled by the UV exposure time. With the contribution of the AIEgenic TPE stopper, the solutions of both [1]rotaxanes and the unthreaded compound in 99% water (DMSO/H_2O = 1/99, v/v) possessed strong blue PL emissions (at 470 nm). Interestingly, DTE ring closure occurred at different extents after UV exposure according to the constraints of their MIM/non-interlocked structures, *i.e.* **[1]RotA**, **[1]RotB** and **NIM** and thus the Förster resonance energy transfer (FRET) phenomena upon UV irradiation could be controlled. Compared with **[1]RotB-O**/**[1]RotB-C** (loosened nano-loops) and **NIM-O**/**NIM-C** (unconstrained linear structures) possessing switchable FRET-OFF/ON behaviours activated by UV/Vis exposures, **[1]RotA** in the acidic condition was FRET-OFF locked and inert to UV exposure due to the larger bending conformation of the DTE p-conformer and a tightened nano-loop. The optimized structures for different forms of [1]rotaxanes **[1]RotA** and **[1]RotB** along with non-interlocked molecule **NIM** calculated by DFT simulations also confirmed the locked/unlocked photochromism of **[1]RotA** (tightening) by acid/base-driven transformation to **[1]RotB** (loosening) as well as to reduce the distance of potentially reactive C1 to C6 for the activation of the ring closure reaction in the DTE moiety. Thus, these dual and sequential locked/unlocked photo-switching effects introduced by multi-stimuli responsive MIMs could be further investigated and the concept of nano-confinement to perform a complex operation might hold potential for the development of programmable molecular machines.

This work is supported by the National Science and Technology Council (grant No. MOST 110-2221-E-A49-003-MY3, 110-2113-M-A49-018 and 111-2634-F-A49-007) and Center for Emergent Functional Matter Science of National Yang Ming Chiao Tung University from The Featured Areas Research Center Program within the framework of the Higher Education Sprout Project by the Ministry of Education (MOE) in Taiwan.

Conflicts of interest

There are no conflicts to declare.

Notes and references

1 H. Tian and Q. C. Wang, *Chem. Soc. Rev.*, 2006, **35**, 361.
2 W. R. Browne and B. L. Feringa, *Nat. Nanotechnol.*, 2006, **1**, 25–35.
3 C. J. Bruns and J. F. Stoddart, *Acc. Chem. Res.*, 2014, **47**, 2186–2199.
4 J. F. Stoddart, *Angew. Chem., Int. Ed.*, 2017, **56**, 11094–11125.
5 Q. C. Wang, D. H. Qu, J. Ren, K. Chen and H. Tian, *Angew. Chem., Int. Ed.*, 2004, **43**, 2661–2665.
6 C. J. Bruns, J. Li, M. Frasconi, S. T. Schneebeli, J. Iehl, H. P. Jacquot de Rouville, S. I. Stupp, G. A. Voth and J. F. Stoddart, *Angew. Chem., Int. Ed.*, 2014, **53**, 1953–1958.
7 S. Yang, C.-X. Zhao, S. Crespi, X. Li, Q. Zhang, Z.-Y. Zhang, J. Mei, H. Tian and D.-H. Qu, *Chem*, 2021, **7**, 1544–1556.
8 S. Amano, S. D. P. Fielden and D. A. Leigh, *Nature*, 2021, **594**, 529–534.
9 S. Chao, C. Romuald, K. Fournel-Marotte, C. Clavel and F. Coutrot, *Angew. Chem., Int. Ed.*, 2014, **53**, 6914–6919.
10 P. Q. Nhien, T. T. K. Cuc, T. M. Khang, C. H. Wu, B. T. B. Hue, J. I. Wu, B. W. Mansel, H. L. Chen and H. C. Lin, *ACS Appl. Mater. Interfaces*, 2020, **12**, 47921–47938.
11 K.-J. Chen, Y.-C. Tsai, Y. Suzaki, K. Osakada, A. Miura and M. Horie, *Nat. Commun.*, 2016, **7**, 13321.
12 A. S. Sanmartin, A. Pastor, A. M. Cuezva and J. Berna, *Chem. Commun.*, 2022, **58**, 290–293.
13 H. Li, J.-N. Zhang, Z. Zhou, H. Zhang, Q. Zhang, D.-H. Qu and H. Tian, *Org. Lett.*, 2013, **15**, 3070–3073.
14 P. Waeles, C. Clavel, K. Fournel-Marotte and F. Coutrot, *Chem. Sci.*, 2015, **6**, 4828–4836.
15 N. Pairault, A. Bessaguet, R. Barat, L. Frederic, G. Pieters, J. Crassous, I. Opalinski and S. Papot, *Chem. Sci.*, 2020, **12**, 2521–2526.
16 M. Dumartin, M. C. Lipke and J. F. Stoddart, *J. Am. Chem. Soc.*, 2019, **141**, 18308–18317.
17 K. Fournel-Marotte and F. Coutrot, *Nat. Chem.*, 2017, **9**, 105–106.
18 S. Garain, B. C. Garain, M. Eswaramoorthy, S. K. Pati and S. J. George, *Angew. Chem., Int. Ed.*, 2021, **60**, 19720–19724.
19 T. T. K. Cuc, P. Q. Nhien, T. M. Khang, C.-C. Weng, C.-H. Wu, B. T. B. Hue, Y.-K. Li, J. I. Wu and H.-C. Lin, *Chem. Mater.*, 2020, **32**, 9371–9389.
20 E. M. G. Jamieson, F. Modicom and S. M. Goldup, *Chem. Soc. Rev.*, 2018, **47**, 5266–5311.
21 S.-J. Rao, K. Nakazono, X. Liang, K. Nakajima and T. Takata, *Chem. Commun.*, 2019, **55**, 5231–5234.
22 S.-J. Rao, Q. Zhang, J. Mei, X.-H. Ye, C. Gao, Q.-C. Wang, D.-H. Qu and H. Tian, *Chem. Sci.*, 2017, **8**, 6777–6783.
23 C. Wang, S. Wang, H. Yang, Y. Xiang, X. Wang, C. Bao, L. Zhu, H. Tian and D.-H. Qu, *Angew. Chem., Int. Ed.*, 2021, **60**, 14836–14840.
24 Q. Zhang, S.-J. Rao, T. Xie, X. Li, T.-Y. Xu, D.-W. Li, D.-H. Qu, Y.-T. Long and H. Tian, *Chem*, 2018, **4**, 2670–2684.
25 M. Irie, T. Fukaminato, K. Matsuda and S. Kobatake, *Chem. Rev.*, 2014, **114**, 12174–12277.
26 S.-Z. Pu, Q. Sun, C.-B. Fan, R.-J. Wang and G. Liu, *J. Mater. Chem. C*, 2016, **4**, 3075–3093.
27 M. Li, L.-J. Chen, Y. Cai, Q. Luo, W. Li, H.-B. Yang, H. Tian and W.-H. Zhu, *Chem*, 2019, **5**, 634–648.
28 R. J. Li, J. J. Holstein, W. G. Hiller, J. Andreasson and G. H. Clever, *J. Am. Chem. Soc.*, 2019, **141**, 2097–2103.
29 W. R. Algar, N. Hildebrandt, S. S. Vogel and I. L. Medintz, *Nat. Methods*, 2019, **16**, 815–829.
30 B. Fang, M. Chu, L. Tan, P. Li, Y. Hou, Y. Shi, Y. S. Zhao and M. Yin, *ACS Appl. Mater. Interfaces*, 2019, **11**, 38226–38231.
31 J. Zhang, R. Zhang, K. Liu, Y. Li, X. Wang, X. Xie, X. Jiao and B. Tang, *Chem. Commun.*, 2021, **57**, 8320–8323.
32 K. Liu, Y. Wen, T. Shi, Y. Li, F. Li, Y. L. Zhao, C. Huang and T. Yi, *Chem. Commun.*, 2014, **50**, 9141–9144.
33 Y. Mao, K. Liu, G. Lv, Y. Wen, X. Zhu, H. Lan and T. Yi, *Chem. Commun.*, 2015, **51**, 6667–6670.
34 R. E. Stratmann, G. E. Scuseria and M. J. Frisch, *J. Chem. Phys.*, 1998, **109**, 8218–8224.
35 A. D. Becke, *J. Chem. Phys.*, 1993, **98**, 5648–5652.
36 C. Lee, W. Yang and R. G. Parr, *Phys. Rev. B: Condens. Matter Mater. Phys.*, 1988, **37**, 785–789.
37 R. Ditchfield, W. J. Hehre and J. A. Pople, *J. Chem. Phys.*, 1971, **54**, 724–728.